Supporting Information

A unique two-phase heterostructure with cubic $NiSe_2$ and orthorhombic $NiSe_2$ for enhanced lithium ion storage and electrocatalysis

Dong Wang[a, b, c*#], Li Li[c#], Zhichao Liu[a*], Shanshan Gao[a], Guangshuai Zhang[a], Yongzhao Hou[a], Guangwu Wen[a, c], Lijuan Zhang[a], Hao Gu[d], Rui Zhang[a*]

[a] *School of Materials Science and Engineering, Shandong University of Technology, Zibo 255000, P. R. China.*

[b] *State Key Laboratory of Advanced Technology for Float Glass, Bengbu 233000, P. R. China.*

[c] *Shangdong Si-Nano Materials Technology Co. Ltd., Zibo 255000, P. R. China.*

[d] *Shanghai Radio Equipment Research Institute, Shanghai 200000, P. R. China.*

[*]Corresponding author.
E-mail address: wangdong2@sdut.edu.cn (D. Wang); liu690047899@163.com (Z. Liu); zrui0810@163.com (R. Zhang)

[#]These authors contribute equally to this work as the first authors.

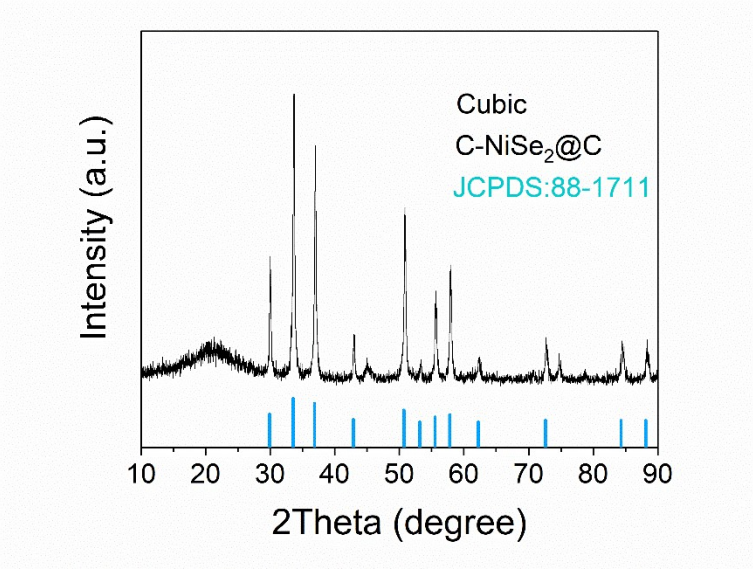

Fig. S1. XRD pattern of the C-$NiSe_2$@C composites

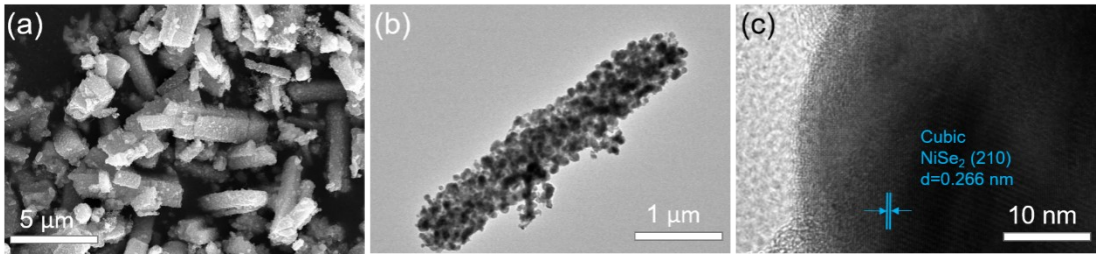

Fig. S2. (a) SEM image, (b) TEM image and (c) HRTEM image of the C-$NiSe_2$@C composites.

The C-$NiSe_2$@C also shows rod-like structure, and the C-$NiSe_2$ nanoparticles can be observed widely distributed within the carbon skeleton.

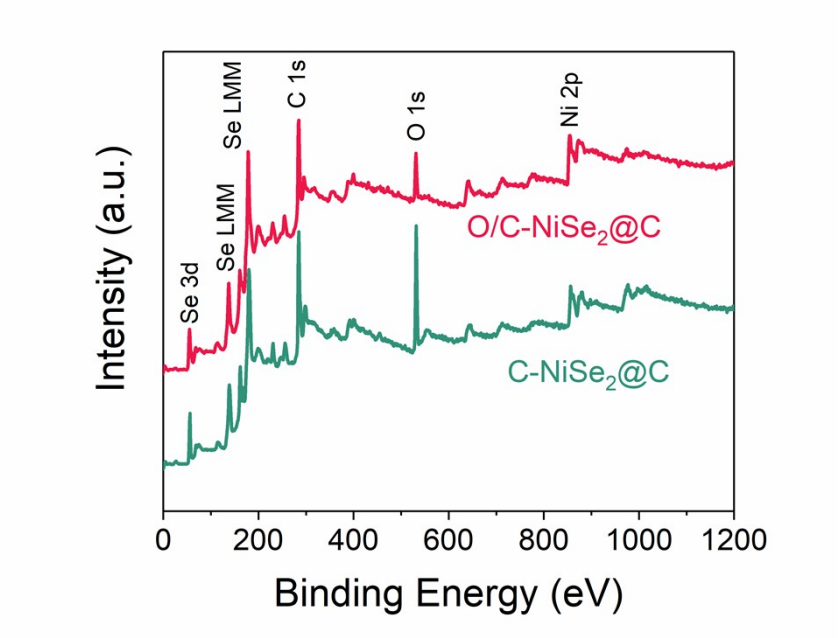

Fig. S3. Survey XPS spectra of the O/C-$NiSe_2$@C and C-$NiSe_2$@C.

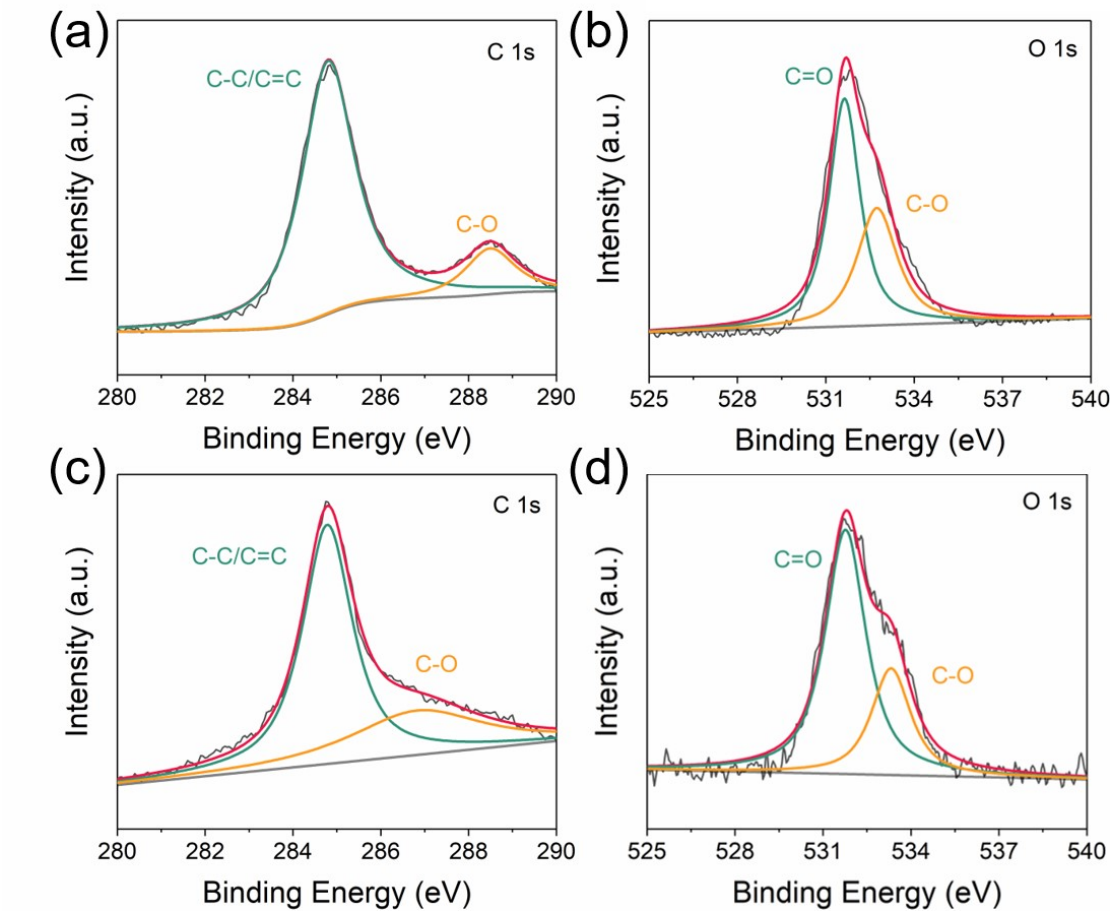

Fig. S4. XPS spectra of (a, c) C 1s and (b, d) O 1s for (a, b) O/C-$NiSe_2$@C and (c, d) C-$NiSe_2$@C.

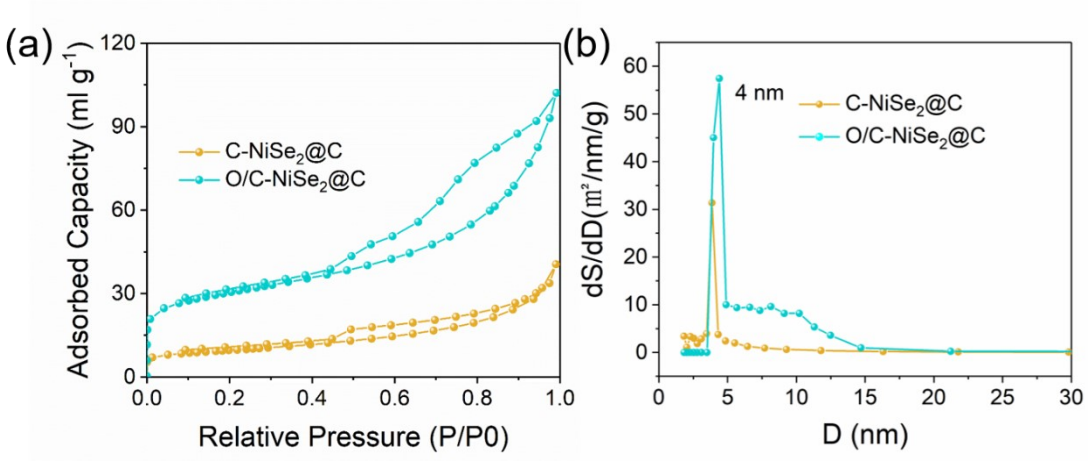

Fig. S5. (a) N_2 adsorption-desorption isotherms and (b) corresponding pore size distribution plots of the two samples

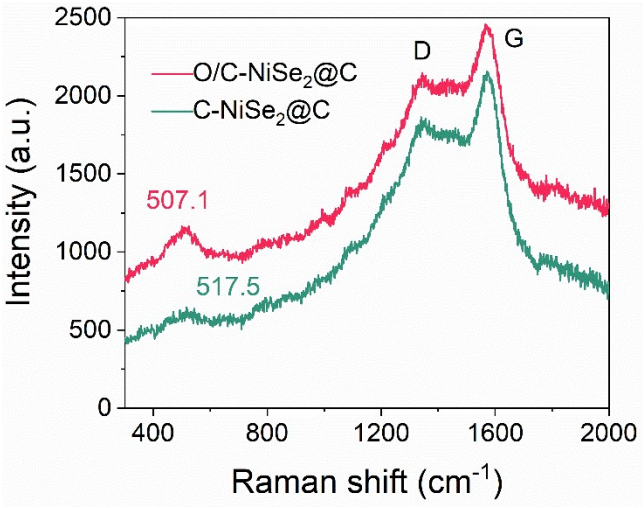

Fig. S6. Raman spectra of the O/C-$NiSe_2$@C and C-$NiSe_2$@C

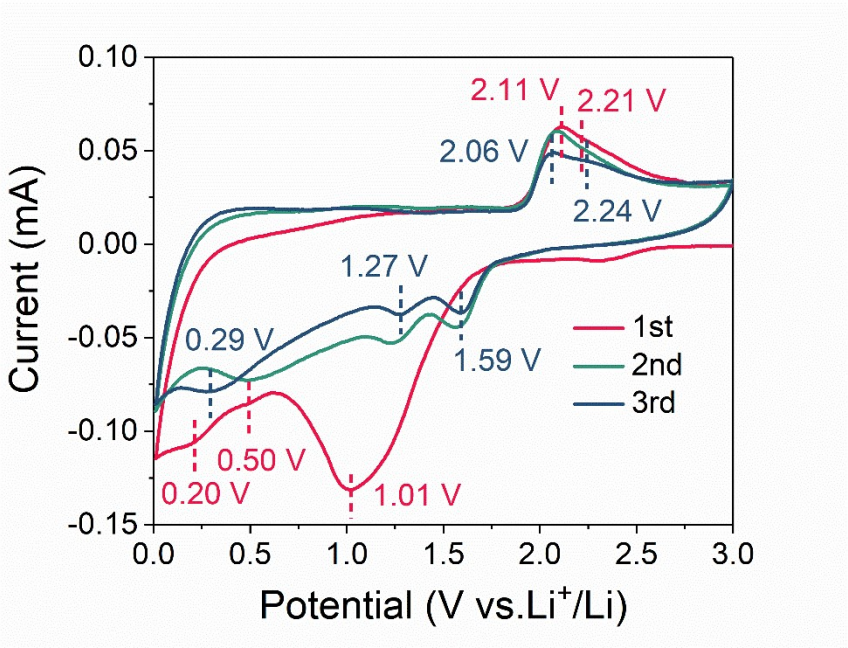

Fig. S7. The initial three CV curves of the C-$NiSe_2$@C at 0.1 mV s^{-1}.

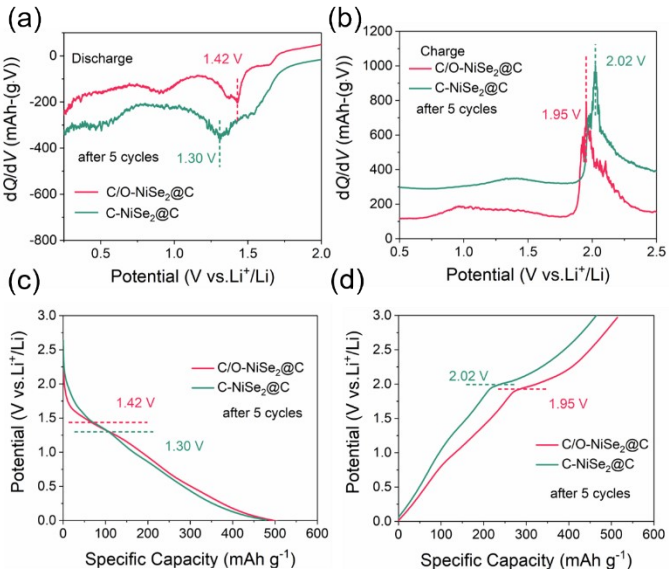

Fig. S8. (a, b) Differential capacity and voltage diagram corresponding to the charge/discharge curve of O/C-$NiSe_2$@C and C-$NiSe_2$@C electrode during (c) discharge and (d) charging processes

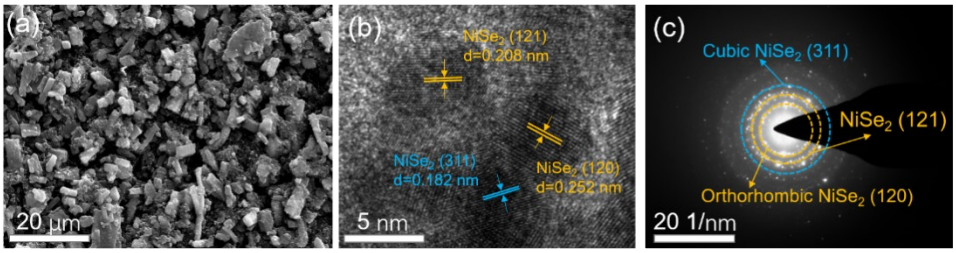

Fig. S9. (a) SEM image after 100 cycles of O/C-$NiSe_2$@C. (b) Ex-situ HRTEM images and (c) corresponding SAED patterns of the O/C-$NiSe_2$@C electrode after the first cycle.

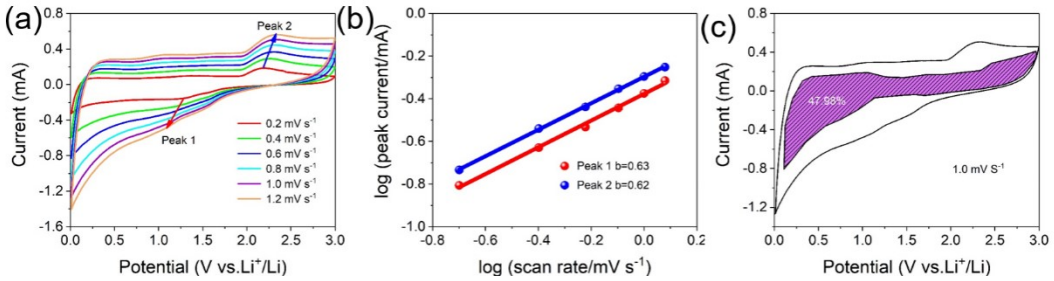

Fig. S10. (a) CV curves of C-$NiSe_2$@C at various scan rates, (b) the corresponding log(i) versus log(v) plots at different redox peaks, and (c) pseudocapacitive contribution (shaded region) at 1.0 mV s^{-1} of C-$NiSe_2$@C.

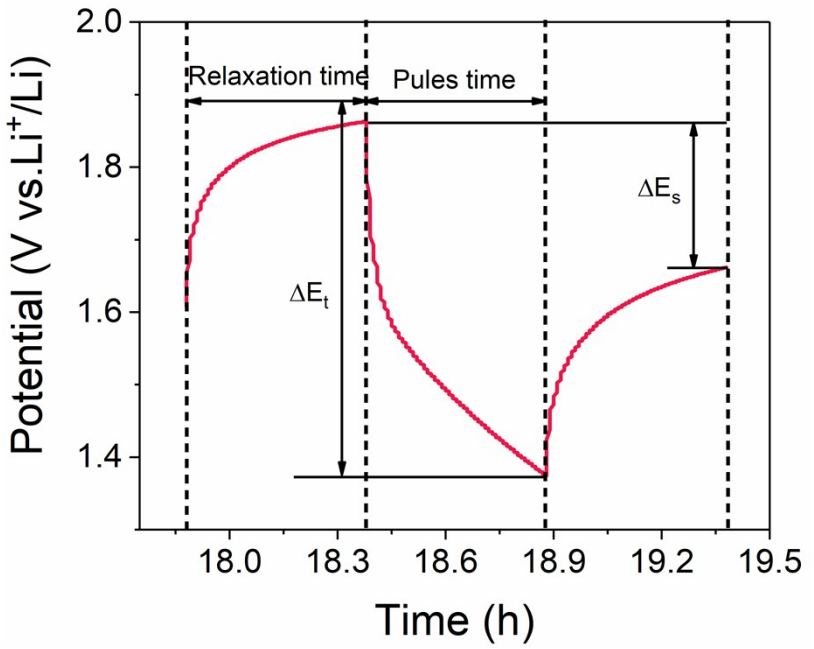

Fig. S11. E vs. t curves of the O/C-$NiSe_2$@C electrode for a single GITT during discharge process.

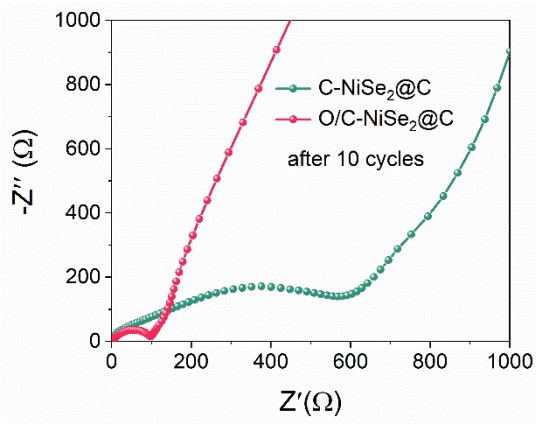

Fig. S12. Nyquist plots of O/C-$NiSe_2$@C and C-$NiSe_2$@C electrodes after 10 cycles.

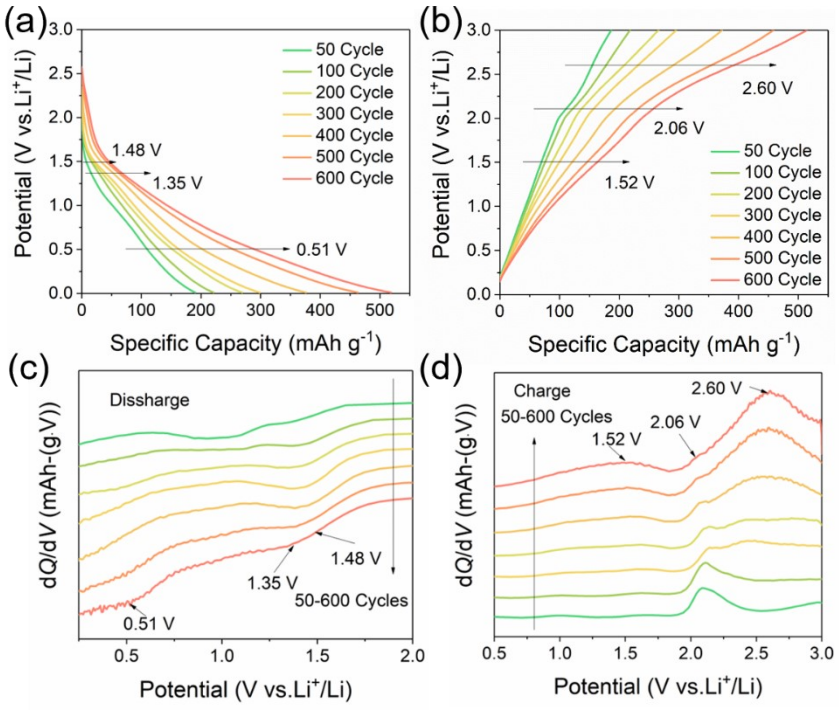

Fig. S13. (a, b) Differential capacity and voltage diagram corresponding to the charge/discharge curve of O/C-$NiSe_2$@C electrode during (c) discharge and (d) charging processes.